Comparative Analysis of Various Classification Algorithms for Skin Cancer Detection

M. Amirjahan
Research Scholar, PG & Research Department of Computer Science, Raja Doraisingam Govt. Art College, Sivagangai, Tamil Nadu, India.

Dr.N.Sujatha
Assistant Professor, PG & Research Department of Computer Science, Raja Doraisingam Govt. Arts College, Sivagangai, TamilNadu, India.

Abstract – Melanoma is one of the skin cancer types that develop the pigment-containing cells refer melanocytes. The collection of Melanoma images plays the major role in skin cancer detection. Traditionally, the enhancement of Melanoma images highlight the affected portion or the defect areas effectively with four methods such as affine detectors-based feature extraction, segmentation of tumorous portions, color constancy and patches. The evolution of automated dermatological diagnostic system supports the medical discipline analysis and the skin anomalies. This paper presents a detailed comparative analysis for classification algorithms used in skin disease analysis. This paper proposes the novel two dependent processes such as skin anomalies detection and disease identification. Initially, high resolution images are gathered from the patient history and proceed the sequential image processing techniques such Gaussian filtering, image enhancement, Gray Level Co-occurrence Matrix (GLCM) feature extraction and the classification. Besides, the comparative analysis between the various classifiers such as C4.5, Support Vector Machine (SVM) and Classification and Regression Trees (CART) to predict the efficient classifier. A novel approach presented in this paper efficiently improves the skin detection and disease identification accuracy compared to existing techniques.

Index Terms – C4.5, CART, Disease Classification, feature Extraction, Gray Level Co-occurrence Matrix (GLCM), Melanoma, Skin Cancer Detection, Support Vector Machine (SVM).

1. INTRODUCTION

Dermatologists faces the major challenge in the skin cancer analysis such as earlier detection of melanomas. The increase in earlier detection improves the patient's survival probability. An efficient in-vivo observation of pigmented skin lesions utilizes the Dermoscopy to increase the early detection rate. The elimination of surface reflection is the major task in the Dermoscopy and it executes prior to the observation. The placement of a magnification instrument on the top of lesion is used to increase the lesion size and a liquid. The Malignant Melanoma (MM) is an aggressive state of the melanocytes that leads to deadly skin cancer. The normal part of the skin called Pigmented Skin Lesions (PSLs) and it specifies the moles or nevi which are closely related to the melanoma. The variations in PSLs are common nevus, blue nevus, dysplastic nevus, congenital nevus and the pigmented spritz nevus. Dysplastic nevi, congentile nevi are the precursors to MM among the PSLs. The major reasons for earlier recognition of Melanoma are listed as follows:

1. Development of melanoma as pre-existing skin lesion
2. Changes in lesion size and color are the major causes of frequent appearing symptoms group.

Fig. 1 shows the melanoma with specific features such as blue whitish (red arrows), pigment networks (blue arrows), dots and globules (white circles).

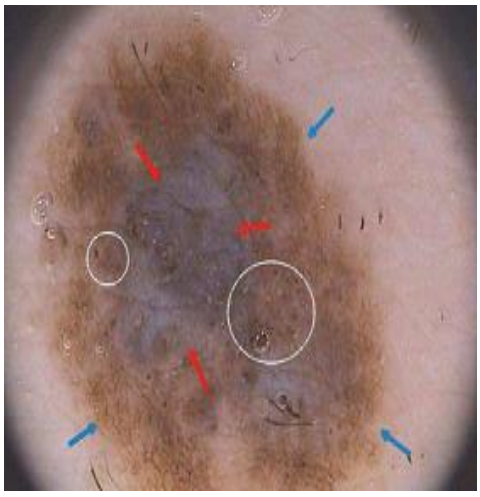

Fig. 1 Melanoma

The detection and classification of global dermoscopic patterns are the major steps to detect the non-melanocytic zones. Testure analysis and classification of lesion patterns utilizes the joint probability and frequency histogram of filter responses for the classification performance improvement. The evolution of Computer Assisted Diagnosis (CAD) systems require the trained professional for early recognition. CAD incorporates the general appearance and global patterns in the lesion order

to perform the diagnosis of malignancy in an earlier manner. The global patterns for the skin lesions are listed as reticular, globular, cobblestone, homogeneous and parallel. CAD provides the future directions to the medical image analysis with the suitable image processing techniques such as enhancement, segmentation, feature extraction and classification. Traditionally, several techniques are used to improve the performance of image processing techniques. Color calibration and normalization techniques are used to improve the image quality. The clustering followed by the active contour segment the image. The numerous features exists in the skin images are color, texture and shape. The features related to Asymmetry, Border irregularity, Color variation, and Diameter (ABCD) is obtained from the ABCD mnemonic rule. Several classification methods ranging from neural network to SVM are available for the characterization of skin lesions. The high-dimensional feature space is the major limiting factor for classifier ability for new data generation. The non-availability of learning algorithm for the data variants leads to the over fitting problems. The analytical identification and extraction of high-level intuitive features are the major stages to quantitatively describe the lesion's symmetry. The built of intuitive features efficiently improve the diagnosis performance and increases the trust level. This paper proposes the novel feature extraction and optimization to increase the classification performance. Besides, this paper investigates the performance of various classifiers to predict the suitable classifier among them.

The rest of the paper is organized as follows. Section II presents a description about the previous research works which is relevant to the skin cancer analysis. Section III involves the detailed description about the proposed skin detection and disease classification models. Section IV presents the performance analysis of proposed and existing methods on parameters. This paper concludes in Section V.

2. RELATED WORK

This section discusses the several related works on dermoscopic images for skin cancer analysis. Barata et al[1] presents the new approach to diagnose the melanomas with the bag of features and the classification based on local small patches. The accessing of discriminative power is depends on the comparison between the color and texture descriptors. The difference between the melanocytic and the melanomas is the necessary stage for skin cancer analysis. Abbas et al [2]proposed the novel classification method in accordance with the color, symmetry and multi-scale texture analysis. Based on the color-texture properties, they proposed the novel pattern optimal classification method for higher accuracy. The most important structure of demoscropy are pigment network and the efficiency of the system was improved by using the automatic system. Barata et al [3]describes the automatic system with the iterative steps as preprocessing, directional filters, adaboost classification. The research work on skin cancer analysis turned to create computerized analysis of Pigmented Skin Lesions (PSLs) for reliable automated system. Korotkov[4]emphasized the estimation of the difference between the demoscropic and clinical image contents. The making of illuminant independent images was performed by using the uniform light source assumption. But, this assumption was violated for real-time images that provided the performance failure in computer vision and object tracking / recognition applications. Varghese and vijay [5]derived the structures for images based on color constancy algorithms and they utilized various light sources for local color correction.

The detection of melanocytic lesions from the non-melanocytic required the detection and classification of global dermoscopic patterns. Sadeghi et al [6]presented the novel approach for texture analysis and the global lesion patterns classification. The utilization of comprehensive set of filter banks on the basis of joint probability distribution function modeled the texture features effectively. Due to the technical complexities and the data scarcities, skin lesion analysis on standard camera images has the immediate attention. Amelard et al [7]presented the measurement of asymmetry of lesion images with the standard cameras. The features correspond to the asymmetry measurement were High-level Intuitive Features (HLIF) and they showed that the low-level statistical features were responsible for skin lesion analysis. Amelard et al [8]applied the multi-stage illumination correction algorithm and defined the High-Level Intuitive Features (HLIF) that quantified the asymmetry level and lesion irregularity. Balleriniet al [9]proposed the novel hierarchical classifier on the basis of K-Nearest Neighbor (K-NN) and discussed its application on the non-melanoma skin lesion classification. The classification task was decomposed into various simple problems termed as hierarchical framework. The embedding of feature selection into the hierarchical framework selected the relevant feature set for classification. The removal of confounding factors from the dermoscopic images was necessary for log-chromocity 2-D color space. The confounding factors were listed as follows: effects of particular characteristics of camera system, color of the light used in dermoscope and the shading. Madooei et al [10]proposed new log-chromaticity 2D color space with an extension of traditional approaches that provide the success in confounding factors removal. They utilized the geometric-mean of color for skin lesion analysis.

The detection and removal of artifacts and the isolation provision between the pigmented lesion and the normal skin were the major issues in the automatic analysis of skin cancer. Madooei et al [11]facilitated the detection and removal of artifacts and presented the effective grey scale conversion approach based on physics and human skin biology. They proposed the grey scale image conversion that provided the high-separability between the pigmented lesion and normal skin surrounding it. The low-cost calibration of demscropic

images was necessary for the color and inconsistency correction. The distortion arised from the chromatic aberration was the variable in magnitude and direction. Wighton et al [12]presented the two low-cost dermoscopes on the basis of consumer-grade cameras. The imaging of the reference and the application of Singular Value Decomposition (SVD) determined the transformation for an accurate color reproduction. The automated computer-aided skin cancer detection based on ABCD rule was the major task focused by the traditional studies. Ramteke et al [13]proposed and explained the automatic detection and analysis of skin cancer by using the ABCD rule. The structural nature of lesion level, wavelet transformation and image decomposition techniques were utilized the watershed segmentation. The diameter estimation based on the Mamdani-based Fuzzy Inference System (FIS) utilized the world recognized the ABCD rule for cancer diagnostic. The solution to the SVM optimization problems depends on the convergence limitation. Chang and Lin [14]presented the libraries of SVM and highlighted the issues in the SVM optimization. The parameters required for an effective classification were estimated from the theoretical convergence limits. The pattern recognition and the machine learning required the considerable attentions in semis supervised approaches. Several semi-supervised learning algorithms were used for binary classification and their extension into the multi-class was governed by using the approach namely one-against-rest. Song et al [15]proposed the semi-supervised learning method with the multi-class boosting capabilities that directly classified the multi-class data and achieved the high classification accuracy. The distinct features used in proposed semi-supervised approach supported the handling of multi-class cases without reduction. The selection of better classification algorithm among the various classification algorithms is investigated in this paper. Besides, this paper provides the improvement in skin cancer detection and disease classification effectively.

3. NOVEL MODEL FOR AUTOMATED SKIN CANCER ANALYSIS

This section discusses the implementation of the proposed model for automated skin cancer analysis. Fig. 2 shows the overall workflow of the proposed work.

The proposed work includes the sequential image processing techniques such as preprocessing, segmentation, feature extraction, optimization and classification. The filtering and enhancement in the preprocessing block improves the quality of the image. The K-means clustering algorithm segments the quality enhanced image and apply the GLCM on feature extraction. The three classification algorithms such as C4.5, CART and SVM are used for the classification of genetic-optimized feature selection.

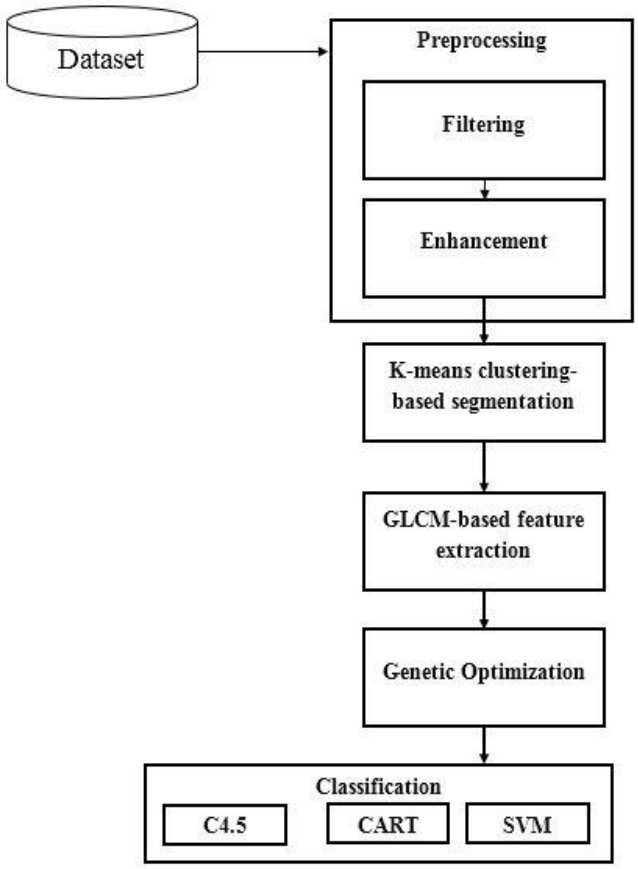

Fig. 2 Overall flow of proposed work

A. Preprocessing

The employment of filtering techniques removes the unwanted or noise components in spatial domain. The interoperability of information exist in an image requires the quality improvement. On the basis of convolution theorem, the frequency domain technique decomposes the image into frequency domain components.

The output of convolution $g(x,y)$ depends upon position variation $h(x,y)$ of an input image $f(x,y)$ described by following equation

$$g(x,y) = f(x,y) * h(x,y) \quad (1)$$

If the$G(u,v)$,$F(u,v)$ and $H(u,v)$ are the transformed output of variables, then the convolution in equation (1) is described by

$$G(u,v) = F(u,v).H(u,v) \quad (2)$$

The working of spatial filters depends upon the neighborhood pixels referred as sub-image. The noise smoothing for a given input image. The weighted sum of intensities of the pixels constitutes the intensity of the pixels in noise smoothened

image. The operation of noise smoothing is governed by following equation

$$\bar{f}(x,y) = \sum_{i=-k}^{k} \sum_{j=-l}^{l} f(x+i, y+j) h(i,j) \quad (3)$$

If the variation of weight values on the kernel function represents the Gaussian coefficients, then the corresponding filter is formed with Gaussian distribution curve. The peak value of Gaussian curve specifies the center of the kernel. The increase in distance from the center pixel decreases the weight values correspondingly. The heavy biased weights towards the center cell and the immediate neighbors in the Gaussian filter preserves the edges. The Sigma parameter σ refers the standard deviation (in numerals) decides the shape of the distribution curve. The large value of sigma assigns more weight to distance cells for greater smoothing and less edge preservation. The function to govern the noise elimination and image smoothening is described as follows:

$$h(x,y) = \frac{1}{2\pi\sigma^2} e^{-\frac{x^2+y^2}{2\sigma^2}} \quad (4)$$

The equation (4) describes Gaussian filter is separable. The Gaussian filtering technique effectively removes the noise samples compared other spatial filters (low and average). Fig. (a) and (b) shows the original and preprocessed images.

(a) (b)

Fig. 3 (a) Original image and (b) Preprocessed Image

The zero-mean noise in an image leads to an effective Gaussian filter. The convolution operation performed in Gaussian filter performed in two ways of either directly or by using FFT. In FFT computation, the difference between the borders (left, right and top, bottom) will raise the artifacts in an image. Hence, direct computation to be preferred.

B. K-means clustering

The unsupervised clustering algorithm (K-means) is efficiently segments the image points into multiple classes with reference to the distance between them. The multiple points are clustered based on the centroid value as μ_i in order to minimize the objective function as

$$V = \sum_{i=1}^{k} \sum_{x_j \in s_i} (x_i - \mu_i)^2 \quad (5)$$

The 2D image is passes through the algorithm to create the segment output. The steps required for K-means based segmentation is listed as follows:

1. Calculate the intensity distribution of (histogram) of the image intensities
2. Initialize the centroids with random intensities computed
3. Repeat the above steps until the clustering labels are not changes
4. Cluster the points based on the distance estimation between the intensities and centroid intensities as follows:

$$c^{(i)} = \arg\min_j \|x_i - \mu_i\|^2 (6)$$

5. Compute the new centroid for each cluster

$$\mu_i = \frac{\sum_{i=1}^{m} 1\{c_{(i)}=j\} x^{(i)}}{\sum_{i=1}^{m} 1\{c_{(i)}=j\}} (7)$$

Fig. 4 shows the clustered objects of skin cancer image

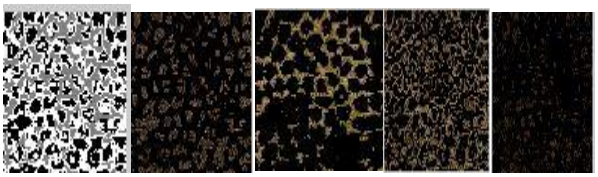

Fig. 3 Clustered objects

C. GLCM-based feature extraction

The analysis of characteristics of texture in response to the non-deterministic properties and the management of relationships between the gray levels of image are necessary. Hence, this paper utilizes the second order textural feature extraction using the Gray-Level Co-occurrence Matrix (GLCM). A matrix that includes the rows and columns representing the gray levels (G) in the image. The element in the matrix ($P_d(i,j\,|\Delta x, \Delta y)$) specifies the relative frequency of two pixels separated by the pixel distance ($\Delta x, \Delta y$). Consider the image includes the number of gray levels (G) with $M \times N$ neighborhood and intensity $f(m,n)$. The matrix element with intensity and gray levels is expressed as

$$P_d(i,j\,|\Delta x, \Delta y) = WQ(i,j\,|\Delta x, \Delta y) (8)$$

Where, $W = \frac{1}{(M-\Delta x)(N-\Delta y)}$

$$Q(i,j\,|\Delta x, \Delta y) = \sum_{n=1}^{n-\Delta y} \sum_{m=1}^{M-\Delta x} A$$

$$A = \begin{cases} 1 & if\ f(m,n) = i\ and\ f(m+\Delta x, n+\Delta y) \\ 0 & Else \end{cases}$$

The computation of features from the matrix manipulation is more computational complexity than the features extraction from the original images. The large dimensionality causes the high sensitivity GLCM and hence the reduction of gray levels are need to be reduced.The estimated probability distribution $P_d(d,\theta)$ contains the simple relationship among the certain pairs. The mean (μ), standard deviation (σ), gray levels (G) and marginal probability matrix ($P_x(i), P_y(j)$) are necessary parameters to extract the textural features (1987) and their relationship with the probability distribution is discussed as follows:

$$P_x(i) = \sum_{j=0}^{G-1} P_d(i,j) \quad (9)$$

$$P_y(j) = \sum_{i=0}^{G-1} P_d(i,j) \quad (10)$$

$$\mu_x = \sum_{i=0}^{G-1} i.P_x(i) \quad (11)$$

$$\mu_y = \sum_{j=0}^{G-1} j.P_y(j) \quad (12)$$

$$\sigma_x^2 = \sum_{i=0}^{G-1}(P_x(i) - \mu_x(i))^2 \quad (13)$$

$$\sigma_y^2 = \sum_{j=0}^{G-1}(P_y(j) - \mu_y(j))^2 \quad (14)$$

By using the basic terms defined from (9) to (14), the textural features $T(i,j)$ are extracted one by one in the following sub-Table 1.

TABLE I GLCM FEATURES

S. No	GLCM features	Equation
1	Contrast	$T_c(i,j) = \sum_{i=1}^{G-1}\sum_{j=1}^{G-1}(i - j)^2 P_d(i,j)$
2	Correlation	$T_{Cr} = \sum_{i=0}^{G-1}\sum_{j=0}^{G-1}\frac{(i \times j) \times P_d(i,j) - (\mu_x \times \mu_y}{\sigma_x \sigma_y}$
3	Cluster prominence	$T_{CP} = \sum_{i=0}^{G-1}\sum_{j=0}^{G-1}(i + j - \mu_x - \mu_y)^4 \times P_d(i,j)$
4	Cluster shade	$T_{CS} = \sum_{i=0}^{G-1}\sum_{j=0}^{G-1}(i + j - \mu_x - \mu_y)^3 \times P_d(i,j)$
5	Dissimilarity	$T_{dis} = \sum_{i=1}^{G-1}\sum_{j=1}^{G-1}\lvert i - j\rvert \times P_d(i,j)$
6	Energy	$T_E = \sqrt{\sum_{i=0}^{G-1}\sum_{j=0}^{G-1} P_d^2(i,j)}$
7	Entropy	$T_{Ent} = \sum_{i=0}^{G-1}\sum_{j=0}^{G-1}(P_d(i,j)) \times \ln(P_d(i,j))$
8	Homogeneity	$T_{hom} = \sum_{i=0}^{G-1}\sum_{j=0}^{G-1}\frac{1}{(i-j^2}P_d(i,j)$
9	Maximum Probability	$T_{MP} = \max_{i,j} P_d(i,j)$
10	Autocorrelation	$T_{AC} = \sum_{i=0}^{G-1}\sum_{j=0}^{G-1}\frac{(i \times j) \times P_d(i,j) - (\mu_x \times \mu_y}{\sigma_x \sigma_y}$

D. Genetic optimization

The search of large space to obtain the relevant features is governed by using the genetic algorithm. The selection of genetic algorithm depends on the insensitive to the noise and hence more robust feature selection is achieved. A form of inductive learning and the adaptive search techniques provide the substantial improvement in feature selection method. The important aspect of the space representation of possible subset of entire feature set is governed by using the binary representation. The overall fitness function required for genetic formulation is defined as the weighted sum of match score of all the recognition as follows:

$$F = \sum_{i=1}^{n} S_i * W_i - \sum_{j=n+1}^{m} S_j * W_j \quad (15)$$

The range of F depends on the number of testing events and associated weights. The normalization of the fitness function by using the total weighed testing samples defined by

$$Fitness = 100 - [(F \,/\, TW) * 100] \quad (16)$$

The subtraction ensures the final evaluation of features selected.

E. Classification

The classification of image features optimized from genetic algorithm includes three algorithms such as C4.5, CART and SVM.

1. C4.5

The construction of decision tree prior to classification is necessary in this process. The node that represents the feature in the tree matches the attribute set and the arc or edge function matches the attribute values range. The informative node for disease depends on the entropy measurement. The node with

larger entropy values considered as informative. The iterative process of nearest neighbor estimation in C4.5 algorithm efficiently removes the unnecessary nodes to produce the shortest tree. The reduction of number of instances will improve the classification performance.

2. CART

For the known correct classification values, the CART identifies and constructs the binary decision tree from the optimized feature set. The root node is formed in such a way that the variable in the feature space minimizes the measure of sibling nodes impurities. The entropy or the impurity measurement are defined as follows:

$$i(t) = -\sum_{j=1}^{k} p(w_j|t) \log p(w_j|t) \quad (17)$$

Where, $p(w_j|t)$ represents the proportion of patterns

w_j represents the class

The non-terminal node is further divided into two levels such as (t_l, t_r). The best division to maximize the difference as

$$\Delta i(s,t) = i(t) - p_L i(t_L) - p_R i(t_R) \quad (18)$$

The successive subdivisions increases the height of decision tree until no significant decrease of the impurity measurement. The stage in which the non-terminal node becomes the terminal node provide the maximum probability values. The node or feature with the maximum probability is the defected image otherwise it is termed as the normal.

3. SVM

According to the statistical theory for image analysis, SVM is the most prominent classification algorithm with maximum accuracy. For the given n training sampes, the input vectors and the output labels are defined as (x_i, y_i). The discriminant function or the classifier function learns the patterns in the training samples efficiently predicts the reliable classification output. The formation of the linear decision boundary or the linear hyperplane between the classes are used for the correct classification of input feature vectors. The optimal hyperplane prediction improves the classification performance further and hence the normalized feature space by using the modified kernel functions predicts the optimal hyperplane are described as

$$SVM\ kernel = \frac{K(\vec{x},\vec{y})}{\sqrt{K(\vec{x},\vec{x})K(\vec{x},\vec{x})}} \quad (19)$$

The mapping of feature vectors to the high dimensional feature space and the creation of separate hyperplane improves the disease classification effectively.

4. PERFORMANCE ANALYSIS

This section discusses the performance validation of classifiers (C4.5, CART and SVM) regarding the accuracy, sensitivity and specificity. The comparative analysis between the classifiers states that the SVM is the best classification technique compared to other. Table II shows the number of positive and negative values for the classification to estimate the basic parameters.

TABLE II

PARAMETRIC EQUATIONS

Parameters	**Descriptions**
True Positive (TP)	Cases of correct classification of diseases
True Negative (TN)	Cases of correct classification of no disease
False Positive(FP)	Cases of incorrect classification of disease
False Negative(FN)	Cases of incorrect classification of no disease.

Table III shows the comparative analysis of classification techniques regarding the sensitivity, specificity and accuracy values.

TABLE III

COMPARATIVE ANALYSIS BETWEEN THE CLASSIFICATION TECHNIQUES

Techniques	**Sensitivity (%)**	**Specificity (%)**	**Accuracy (%)**
C4.5	96.12	85.3	92.5
CART	95.1	88.4	93.4
SVM	96.1	83.6	94.3

The overall accuracy is the measure of effectiveness of classification algorithms. It is defined as the overall correct classification of defected and normal images to the total number of images as follows:

$$Accuracy = \frac{TP+TN}{TP+TN+FP+FN} \quad (20)$$

The sensitivity of the classification is defined as follows:

$$sensitivity = \frac{TP}{TP+FN} \quad (21)$$

The specificity of the classification is defined as follows:

$$specificity = \frac{TN}{TN+FP} \quad (22)$$

Fig. 5 shows the parametric variations for C4.5, CART and SVM classifiers. The accuracy values are 92.5, 93.4 and 94.3 % respectively.

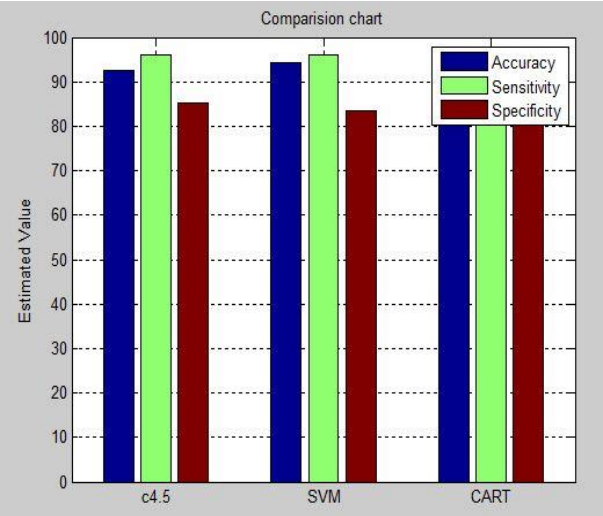

Fig. 5 Parametric analysis

The comparative analysis shows the SVM classifier provides the 1.91 and 0.95 % improvement in accuracy compared to C 4.5 and CART respectively. The sensitivity values are 96.12, 95.1 and 96.53 % respectively. The comparative analysis shows the SVM classifier provides the 0.4 and 1.48 % improvement in sensitivity compared to C 4.5 and CART respectively. The specificity values are 85.3, 88.4 and 83.6 % respectively. The comparative analysis shows the SVM classifier provides the 1.99 and 5.43 % deviationin specificity compared to CART and C 4.5 respectively.

5. CONCLUSION

The collection of Melanoma images played the major role in skin cancer detection. Traditionally, the enhancement of Melanoma images highlighted the affected portion or the defect areas effectively with four methods such as affine detectors-based feature extraction, segmentation of tumorous portions, color constancy and patches. The evolution of automated dermatological diagnostic system supported the medical discipline analysis and the skin anomalies. This paper presented the detailed comparative analysis for classification algorithms used in skin disease analysis. This paper proposed the novel two dependent processes such as skin anomalies detection and disease identification. Initially, high resolution images are gathered from the patient history and proceed the sequential image processing techniques such Gaussian filtering, image enhancement, Gray Level Co-occurrence Matrix (GLCM) feature extraction and the classification. Besides, the comparative analysis between the various classifiers such as C4.5, Support Vector Machine (SVM) and Classification and Regression Trees (CART) predicted the efficient classifier. A novel approach presented in this paper efficiently improved the skin detection and disease identification accuracy compared to existing techniques.

REFERENCES

[1] C. Barata, M. Ruela, T. Mendonça, and J. S. Marques, "A bag-of-features approach for the classification of melanomas in dermoscopy images: The role of color and texture descriptors," in *Computer vision techniques for the diagnosis of skin cancer*, ed: Springer, 2014, pp. 49-69.

[2] A. Chakrabarti, K. Hirakawa, and T. Zickler, "Color constancy with spatio-spectral statistics," *IEEE Transactions on Pattern Analysis and Machine Intelligence*, vol. 34, pp. 1509-1519, 2012.

[3] C. Barata, J. S. Marques, and J. Rozeira, "A system for the detection of pigment network in dermoscopy images using directional filters," *IEEE transactions on biomedical engineering*, vol. 59, pp. 2744-2754, 2012.

[4] K. Korotkov and R. Garcia, "Computerized analysis of pigmented skin lesions: a review," *Artificial intelligence in medicine*, vol. 56, pp. 69-90, 2012.

[5] A. Varghese and D. Vijay, "Improving Edge Based Color Constancy for Multiple Light Sources."

[6] M. Sadeghi, T. K. Lee, D. McLean, H. Lui, and M. S. Atkins, "Global pattern analysis and classification of dermoscopic images using textons," in *SPIE Medical Imaging*, 2012, pp. 83144X-83144X-6.

[7] R. Amelard, J. Glaister, A. Wong, and D. A. Clausi, "Melanoma decision support using lighting-corrected intuitive feature models," in *Computer Vision Techniques for the Diagnosis of Skin Cancer*, ed: Springer, 2014, pp. 193-219.

[8] R. Amelard, A. Wong, and D. A. Clausi, "Extracting high-level intuitive features (HLIF) for classifying skin lesions using standard camera images," in *Computer and Robot Vision (CRV), 2012 Ninth Conference on*, 2012, pp. 396-403.

[9] L. Ballerini, R. B. Fisher, B. Aldridge, and J. Rees, "A color and texture based hierarchical K-NN approach to the classification of non-melanoma skin lesions," in *Color Medical Image Analysis*, ed: Springer, 2013, pp. 63-86.

[10] A. Madooei, M. S. Drew, M. Sadeghi, and M. S. Atkins, "Automated Pre–processing Method for Dermoscopic Images and its Application to Pigmented Skin Lesion Segmentation," in *Color and Imaging Conference*, 2012, pp. 158-163.

[11] A. Madooei, M. S. Drew, M. Sadeghi, and M. S. Atkins, "Intrinsic melanin and hemoglobin colour components for skin lesion malignancy detection," in *International Conference on Medical Image Computing and Computer-Assisted Intervention*, 2012, pp. 315-322.

[12] P. Wighton, T. K. Lee, H. Lui, D. McLean, and M. S. Atkins, "Chromatic aberration correction: an enhancement to the calibration of low-cost digital dermoscopes," *Skin Research and Technology*, vol. 17, pp. 339-347, 2011.

[13] N. S. Ramteke and S. V. Jain, "ABCD rule based automatic computer-aided skin cancer detection using MATLAB®," *International Journal of Computer Technology and Applications*, vol. 4, p. 691, 2013.

[14] C.-C. Chang and C.-J. Lin, "LIBSVM: a library for support vector machines," *ACM Transactions on Intelligent Systems and Technology (TIST)*, vol. 2, p. 27, 2011.

[15] E. Song, D. Huang, G. Ma, and C.-C. Hung, "Semi-supervised multi-class Adaboost by exploiting unlabeled data," *Expert Systems with Applications*, vol. 38, pp. 6720-6726, 2011.